Received: 26 September 2018 | Accepted: 7 December 2018

DOI: 10.1002/pcr2.10053

WILEY Polymer Crystallization

PERSPECTIVES

A few rediscovered and challenging topics in polymer crystals and crystallization

Kan Yue[1] | Gengxin Liu[2] | Xueyan Feng[3] | Liangbin Li[4] | Bernard Lotz[5] | Stephen Z. D. Cheng[1,3]

[1]South China Advanced Institute for Soft Matter Science and Technology, South China University of Technology, Guangzhou, China

[2]Center for Advanced Low-dimensional Materials, Donghua University, Shanghai, China

[3]College of Polymer Science and Polymer Engineering, The University of Akron, Akron, Ohio

[4]National Synchrotron Radiation Lab and CAS Key Laboratory of Soft Matter Chemistry, University of Science and Technology of China, Hefei, China

[5]Institut Charles Sadron, CNRS-Universite de Strasbourg, Strasbourg, France

Correspondence
Stephen Z. D. Cheng, South China Advanced Institute for Soft Matter Science and Technology, South China University of Technology, Guangzhou 510640, China.
Email: scheng@uakron.edu
and
Bernard Lotz, Institut Charles Sadron, CNRS-Universite de Strasbourg, 23 Rue du Loess, 67034 Strasbourg, France.
Email: bernard.lotz@ics-cnrs.unistra.fr
and
Liangbin Li, National Synchrotron Radiation Lab and CAS Key Laboratory of Soft Matter Chemistry, University of Science and Technology of China, Hefei 230026, China.
Email: lbli@ustc.edu.cn

Funding information
Fundamental Research Funds for the Central Universities in SCUT, Grant/Award Number: 2017JQ001; National Science Foundation, Grant/Award Number: DMR-1408872; Pearl River Talents Scheme of Guangdong (CN), Grant/Award Number: 2016ZT06C322

Abstract

This feature article discusses a few rediscovered and challenging topics in polymer crystals and crystallization. Among many research topics in this field, primary nucleation of polymers, twisted and curved polymer crystals, flow-induced crystallization, and supramolecular crystals are selected and illustrated. This selection includes traditional topics with yet to be solved critical questions, and relatively new topics that still call for more developments. Specific attention is paid to the supramolecular crystallization of a new class of macromolecules termed "giant molecules," which show unusual self-assembly behaviors toward diverse hierarchical nanostructures. We believe that although being an old topic of long history, study on polymer crystallization will continue to flourish and will contribute to a more comprehensive understanding of self-assembly in polymers.

KEYWORDS

curved polymer crystals, flow-induced crystallization, giant molecules, polymer crystals, supramolecular crystals

1 | INTRODUCTION

Research on polymer crystals and polymer crystallization has a long history that can be traced back to well over half a century ago. Grown with modern polymer science, we have witnessed the birth and booming of this field, which has been perhaps the most investigated, prolonged and successful research field. When looking back, this research field was new and revolutionary at that time, featuring extreme activeness and dynamics. However, even if we ask today, "have the major questions in crystalline polymers been solved?", a short answer would be: "No, not by a long shot." As illustrated by Lovinger,[1] "what happened is that some of the unsolved problems have led to intense controversies or dead ends, and researchers in crystalline polymers have focused their attention more and more on ever narrower problems and ever more specialized materials. Most of us have been cultivating our own "trees of knowledge," working on our favorite polymers, properties, or techniques. Sometimes our efforts extend beyond these individual "trees" and build a little "grove" as we address, for example, families of related polymers or properties of greater breadth. But, as the saying goes, we generally keep missing the forest for the "trees".[1]

Further questions may include: Why could this research field be extended for such a long time? What is the driving force for investigating polymer crystals and polymer crystallization? One apparent reason could be that nearly two-thirds of commercialized polymers are crystalline polymers, and the applications of these polymers are so extensive

and pervasive as they range from our daily lives to high-technologies. A second reason is simply that many research topics have been long-lasting in nature, not only because of the complicity of these subjects themselves, but also because of the ever-renewed needs of new materials and structures for emerging applications. From a practical point of view, current hot topics in the field of polymer crystals and polymer crystallization include: effects of controlled polymer architecture on processing polymer crystals and crystallization; bulk property dependency on crystallinity and morphology; anisotropic structures and properties of low-dimensional polymers (such as fibers, films, and membranes); crystalline polymer blends and compound formulations; effects of nucleation agent on mechanical and optical properties; and many others.

Scientifically, early major discoveries in this field include the observation and description of polymer crystalline spherulites in the early 1950s;[2,3] discovery of lamellar single crystals in solution and in the melt in the 1950s;[4–6] heated discussions on the validity and extent of chain folding;[6,7] crystal structures and symmetry, crystal habits and morphologies,[8,9] and so on. Study on polymer crystals and crystallization has also been stimulated by the intense experimental investigation and debates over crystal-growth models;[10,11] polymer crystal annealing and melting;[12] crystal defects and interfaces;[12] crystalline polymers blends, copolymers and hybrids;[13,14] polymer crystallization under confined and low-dimensional environments;[15,16] and the elucidation and exploitation of a variety of physical properties. Besides, new crystalline polymers have been continuously synthesized with various new structures and for designed applications. Recently, the concept of supramolecular crystals and crystallization is emerging along with the development of unconventional hierarchical structures building upon ordered assemblies of small molecules and macromolecules via delicate noncovalent interactions.

After 70 years of continued investigation in this field, what are the pathways that would allow us to correctly go through this "forest of trees" and reach our ultimate goal in understanding fundamentals of polymer crystals and crystallization? One of the key issues is how to recognize a quantitative description of the metastable nature of polymer crystals and how to understand the paths to form polymer crystals during crystallization.[17] In this feature article, we would like to focus our attention on a few key concepts and rediscovered and challenging topics, which are fundamentally important for our understanding of this field including polymer primary nucleation, twisted and curved polymer crystals, crystallization during deformation, and supramolecular crystals.

2 | PRIMARY NUCLEATION AND CRYSTAL GROWTH

A classical crystal refers to a homogenous solid with constituents packed into an ordered microscopic structure unit (or a motif), which periodically repeats exactly identical arrangements according to a crystal lattice in the three-dimensional (3D) space.[18] A motif, as the smallest repeating building block, can be composed of atoms, ions, parts of a molecule, a whole molecule, or even a group of molecules. The most important characteristics of a crystal is that it possesses long-range positional, bond-orientational, and molecular orientational orders with respect to the arrangement of its motif. Information about crystal lattice is usually obtained by X-ray and/or electron diffraction experiments, which, based on the Bragg equation, provides the reciprocal lattice of the crystal lattice in real space. It is thus evident that a reciprocal lattice is a Fourier transformation of its corresponding real-space lattice.[18]

2.1 | Crystal nucleation

As an essential question about crystals, people naturally wonder how a crystal forms. It is now widely accepted that the formation of a crystal must be started with a very small baby crystal termed as "nucleus." A nucleus always first forms for crystallization of both small molecules and polymers, even in a supercooled liquid away from thermodynamic equilibrium. In 1878, Josiah Willard Gibbs proposed a new concept called "surface energy," defined as the work needed to create a unit area of new surface.[18] This concept has been decisively applied in studying crystallization, since the formation of a crystal is associated with two opposite thermodynamic terms: a negative term of bulk Gibbs free energy that stabilizes the crystal, and a positive term of surface free energy as new surfaces are created in the formation of this crystal, which destabilizes the crystal. Considering the competition between these two terms, the surface free energy wins at the initial stage when the crystal (or nucleus) is small, which represents a process with a positive overall Gibbs free energy called nucleation barrier. Only when the crystal size is big enough, the bulk Gibbs free energy term becomes dominant and the overall crystal becomes stable to allow for continuous growth.

Since then, many different versions of nucleation barriers have been proposed, yet in principle, all of them are based on the concept of "surface energy" proposed by Gibbs. Actually, the general formula for the nucleation barrier is quite simple and can be written as

$$\Delta G = -V\Delta g_f + A\gamma + B\gamma_e \quad (1)$$

where ΔG is the Gibbs free energy difference between the initial (isotropic liquid) and the final (crystal) states, and is thus the driving force for the crystallization process; Δg_f is the bulk Gibbs free energy change with a crystal volume of V; and γ and γ_e are the lateral and fold-surface free energy densities, and A and B are the lateral and fold-surface areas, respectively. This nucleation barrier is a determining factor for the nucleation rate (i) following the relationship of

$$i = \left(\frac{NkT}{h}\right) exp\left\{\frac{-(\Delta G + \Delta G_\eta)}{(kT_x)}\right\}, \quad (2)$$

where h is the Planck constant, N is the number of uncrystallized molecules that can participate in the nucleation process, and T_x is the temperature at which crystallization takes place. The terms ΔG and ΔG_η are the nucleation barrier defined by Equation 1 and the free energy of activation related to molecular mobility across the phase boundary, respectively.

Now it is clear that crystal growth follows the completion of the nucleation process. How do we describe this growth process? Would the crystal grow spontaneously and continuously? Tammann proposed in 1903 that crystal growth could be defined as a surface nucleation related process after the first nucleation step (called primary nucleation). It was then predicted that these two processes would show

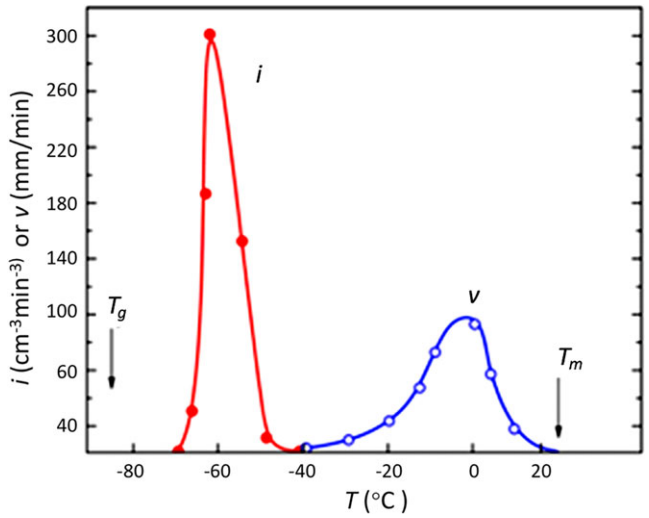

FIGURE 1 Temperature dependence of primary nucleation (red) and linear growth (blue) rates in crystallization of glycerol. T_m and T_g are the melting temperature and glass transition temperatures of glycerol, respectively.
Adapted with permission from Ref. [18]

different supercooling dependence. The primary nucleation would occur at a lower crystallization temperature (higher supercooling) region, whereas the surface nucleation would take place at a higher crystallization temperature (lower supercooling) region. This prediction has been confirmed by a study on the crystallization of a small molecule, glycerol, as shown in Figure 1. However, this type of figure is much more difficult to plot in polymer crystallization, because of the experimental difficulties to completely separate the homogeneous and heterogeneous nucleation processes in the primary nucleation step.[17,18]

The first quantitative study on primary nucleation was reported by Vonnegut in 1948, which is known as the "droplet experiment" today.[20] Vonnegut et al. designed a method to disperse an isotropic melt into small droplets with a few micrometers in size. Such droplets were so small that only a small portion of droplets contained a single heterogeneous nucleus, whereas other droplets contained no heterogeneous nucleus. When those liquid droplets were quenched to low temperatures for crystallization, two situations were possible: Crystallization was initiated by the heterogeneous nucleus for the former case, or a homogeneous nucleus formed in each droplet without any heterogeneous nucleus. Using this design, it was possible to differentiate the homogeneous and heterogeneous nucleation processes in crystallization.

For polyethylene (PE) droplets with sizes ranging from 1 to 3 μm, four different nucleation processes were clearly identified during cooling at a rate of 0.17°C/min (Figure 2).[19] Above 125°C, no nucleation and crystallization could take place. Between 125°C and 100°C, only 5% of all the droplets, which had larger sizes and heterogeneous nucleus inside, were solidified. Between 100°C and 87°C, both heterogeneous and homogeneous nucleation could occur, and more than 50% of the droplets were crystallized at 87°C. When cooled below 85°C, homogeneous nucleation dominated. The kinetics of droplet crystallization could be quantified under isothermal crystallization conditions by using the number ratio of crystallized and overall droplets (n/n_0) and half-time ($t_{1/2}$) of a crystallized droplet at a specific crystallization temperature.

Although elegantly designed, the uncertainty of the droplet experiments is reflected in several aspects. One major concern is about the micrometer size and uniformity of these droplets. Based on the study of crystallization under confined environments, it was later evident that a much smaller space was needed to carry out a single nucleation event, indicating the necessity for droplets with sub-micrometer sizes. Until more than 50 years later, in 2003, Dalnoki-Veress et al. reported a modified version of the droplet experiments using sub-micro-sized polymer melt droplets.[21] They coated a nanometer thick film of poly(ethylene oxide; PEO) on a polystyrene (PS) surface. Because of the incompatibility of the two polymers, when melted, the PEO thin film starts dewetting on the PS surface and forms sub-micro-sized droplets. Each droplet hosts no, or only a single nucleus. As shown in Figure 3A, under similar cooling or isothermal crystallization conditions, crystallization of such sub-micro-sized PEO droplets can be followed by using polarized light microscopy (PLM).[21] From this study, it is found that the homogeneous nucleation takes place at −2°C for a "clean" PEO sample with only few foreign particles acting as heterogeneous nuclei (Figure 3C).[21,22] Even for "dirty" PEO samples, the heterogeneous and homogeneous nucleation processes could be clearly distinguished (Figure 3B). This experimental approach provides a powerful means to study primary nucleation and crystallization kinetics of polymers.

The next interesting question about polymer crystallization is: How does the primary nucleation affect the overall crystallization process? A study on isothermal crystallization of isotactic PS (*it*-PS), which is a crystalline polymer with extremely slow crystallization rates, is illustrated in Figure 4.[23] Two different routes for the isothermal crystallization process were investigated. In the first route, an isotropic melt of isotactic PS was directly quenched to a fixed crystallization

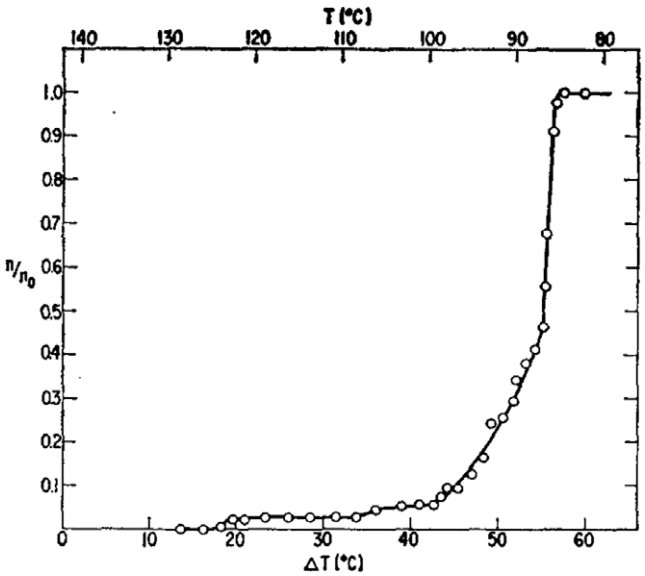

FIGURE 2 Plot of number fraction of polymer droplets solidified vs temperature. Cooling rate: 0.50°C/min above 100°C and 0.17°C/min below 100°C.
Reproduced with permission from Ref. [19]; copyright 1962 AIP Publishing

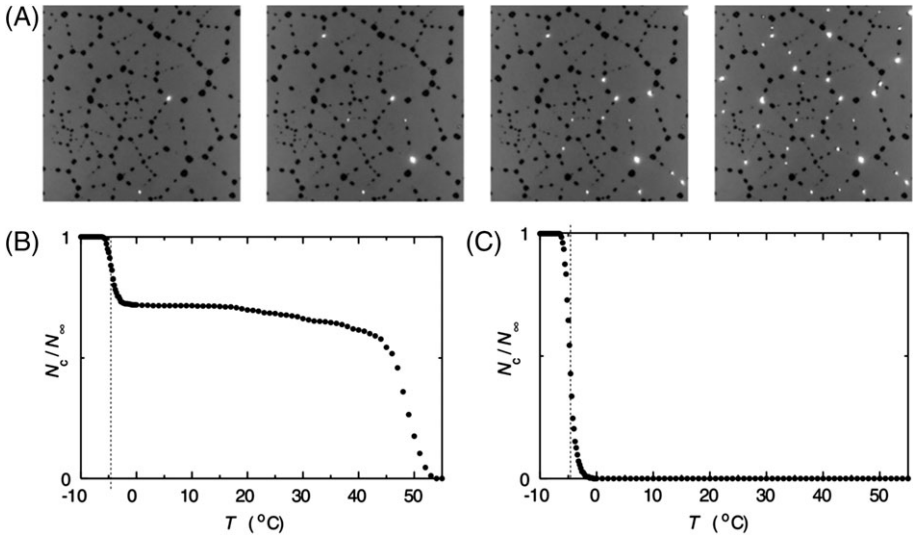

FIGURE 3 (A) PLM images showing crystallization of sub-micro-sized PEO droplets during cooling at 0.4°C/min starting at T_x = −2°C for the first image. The temperature interval between neighboring images is 0.6°C. Dark droplets are amorphous, whereas white droplets are semi-crystalline. Each image is 1000 μm wide. (B,C) Plot of the fraction of crystalized droplets (N_c/N_∞) as a function of temperature for a sample with (B) a high and (C) a low content of heterogeneous nucleus during cooling at 0.4°C/min.
Adapted from Ref. [21] with kind permission of The European Physical Journal (EPJ); copyright 2003 EDP Sciences, Società Italiana di Fisica, and Springer-Verlag

temperature (T_x); whereas in the second route, the melt was quenched to 70°C (below its glass transition temperature, T_g, of 100°C) and aged for six minutes, before rapidly heating to the same fixed crystallization temperature (T_x).

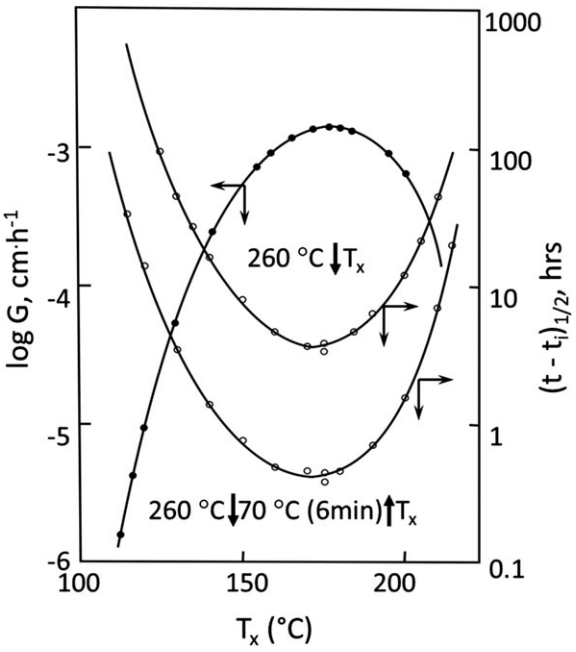

FIGURE 4 Temperature dependence of linear crystal growth rate (line with closed circles) and overall crystallization half-times of *it*-PS (lines with open circles). Two different thermal histories were studied: One sample was directly quenched from the isotropic melt at 260°C to different T_x (upper line with open circles); and the other sample was first quenched to 70°C and annealed for 6 minutes before returned to T_x (lower line with open circles).
Reproduced with permission from Ref. [23]; copyright 2005 Elsevier Ltd

At the same crystallization temperature, the crystal growth rates for both routes measured by PLM were not affected by the thermal history differences. However, the crystallization half-times of samples following different thermal treatment routes, which represented the overall crystallization rates and could be measured by differential scanning calorimetry, differed by one decade of time. Samples following the second route crystalized much faster than those in the first route. The increase in overall crystallization rate could be mainly attributed to an increase of primary nucleation density by nearly three orders of magnitude.

To understand the significantly increased primary nucleation density observed in the second route, two possible primary nucleation events, one at slightly above T_g during cooling and the other at 70°C (below T_g) during aging, should be distinguished. This can be achieved by conducting experiments with changed aging times at 70°C and extrapolating the aging time to zero to obtain a theoretical overall crystallization rate without aging. If this rate matched the rate determined from the first route with direct quenching of the isotropic melt, the primary nucleation thus takes place during the aging rather than during the quenching. These results could bring in additional interesting questions: Since the large-scale thermal fluctuation is frozen below T_g, how are the local densifications developed during aging in an undercooled liquid and thus, the undercooled liquid becomes a heterogeneous system? Furthermore, how do the local densifications contribute to promoting the primary nucleation process? These are still open questions that deserve further investigation.

2.2 | Crystal growth

As revealed by many theoretical approaches, the crystal growth step after primary nucleation has been recognized as a surface nucleation-controlled process. However, this kinetic mechanism holds only when the crystal growth takes place on an atomically smooth surface. In this

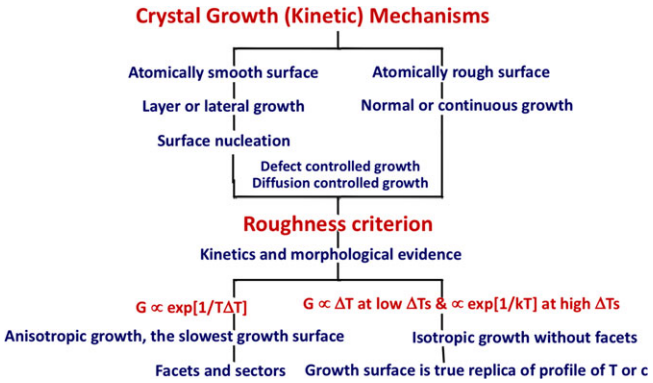

FIGURE 5 A summary of crystal growth mechanisms and their experiential evidence

case, a surface nucleation step with a nucleation barrier is required. Experimentally, this surface nucleation-controlled process is supported by the fact that crystal growth rates exhibit an exponential dependence with respect to both the nucleation barrier and the free energy of activation (ΔG_η). In particular, for growths of single crystals, the issue of nucleation control can be judged by analyzing single crystal habit. A nucleation-controlled single crystal growth results in well-defined macroscopic facets with sectors formed, since faceted single crystal growth is always determined by the slowest crystal growth planes. Formation of faceted single crystals is also known as lateral growth with a surface nucleation process in dilute or condensed states.

Several extensions of the nucleation and growth model have been considered. In a recent development, the rates of attachment of stems during the so-called lateral spread differ on the opposite sides of the primary nuclei in order to take in account the asymmetry of the deposition sites for low symmetry unit-cell (other than tetragonal or hexagonal).[24,25] The calculated resulting crystal growth faces shapes correspond to segments of ellipses the centers of which are no longer centered but shifted laterally on the growth faces. With these additional parameters, the various crystal shapes of diverse polymer crystals (long alkanes, PEO, poly(vinylidene fluoride) [PVDF],...) formed under different conditions (bulk, solution,...) have been reproduced.[24,25] In addition, the basic assumption of uneven lateral spread is supported by the asymmetric single crystal shapes observed for the frustrated, asymmetric crystal structure of isotactic poly(2-vinylpyridine).[26]

Conversely, a fundamentally different growth kinetics, known as the continuous growth model, is proposed to deal with crystal growths on an atomically rough surface. In this model, it is visualized that ledges, corners and holes that exist on rough surfaces can naturally serve as preferred impingement sites for molecular depositions. As a result, the surface nucleation barrier can be ignored. Furthermore, since every impingement site is a potential growth site, surface diffusion is not important, neither. Based on this physical model, a linear relationship between the growth rate and the undercooling ($\Delta T = T_m - T_x$, where T_m is the equilibrium melting temperature) can be predicted, and the growth rate exhibits an exponential dependence on the free energy of activation ΔG_η.

Following the continuous growth model, the single crystal habits are controlled by profiles of concentration and/or temperature during crystallization. Therefore, the shape of a single crystal is a true replica of the concentration and/or temperature gradients, but not a representative of the crystallographic growth planes. Curved crystals are often observed, which are indirect indications of the continuous growth mechanism. But it should be noted that this indication is not sufficient. In other words, although the continuous growth mechanism indeed cannot produce faceted crystal habits, the absence of macroscopic facets in curved single crystal habits does not necessarily imply that the system follows the continuous growth mechanism.

The critical issue between these two different growth models is the roughness of the crystal growth front. What is the critical degree of growth surface roughness that would switch the crystal growth behavior from one mechanism to the other? This roughness criterion is clearly defined in crystallization of small molecules. A quantitative assessment in polymer crystallization has yet to be achieved. Figure 5 summarizes various crystal growth mechanisms for the readers' convenience. Beyond these general descriptions of a crystallization process, some more detailed approaches are also proposed based on two different sets of experimental observations: either from the structural and/or morphological or the scattering data.[2] These two viewpoints have led to dissimilar models for detailed microscopic descriptions of polymer crystallization, although all of these theoretical models are kinetic in nature.

Despite of all the intense investigations for the past 70 years, major issues and questions still remain in polymer crystallization and are yet to be resolved: (1) For example, a complete understanding of the microscopic structure and dynamics of supercooled liquids is still lacking. Fundamental questions like “are supercooled liquids homogeneous?” remain unclear. (2) Current theoretical models in analytical forms all adopt mean-field approaches and thus, they lose the details of molecular dynamic pathways during crystallization, yet the specific trajectory of one individual polymer chain during crystallization may be very different from others. As a result, although the current models may provide reasonable explanations for a majority of experimental results reported so far, they cannot yet predict new crystallization behaviors and (3) Questions about the microscopic and dynamic aspects of nucleation and crystal growth. After all, what is the nucleation barrier? Obviously, this free energy barrier must have both enthalpic and entropic origins, which are critically associated with the molecular structure and chain dynamics at microscopic length scales. But how exactly does a polymer chain with a 3D random coil conformation convert into predominately chain-folded lamellar crystals?[23,27,28] Likewise, people have also asked what would happen after the nucleation barrier is overcome? Whether the crystal could grow spontaneously and freely to a macroscopic scale size? Seeking for answers to these questions would further advance our understanding of polymer crystals and crystallization.

3 | TWISTED AND CURVED POLYMER CRYSTALS CAUSED BY UNBALANCED SURFACE STRESSES

It is a difficult and complex task to experimentally recognize and analyze unbalanced surface stresses in chain folded lamellar crystals.

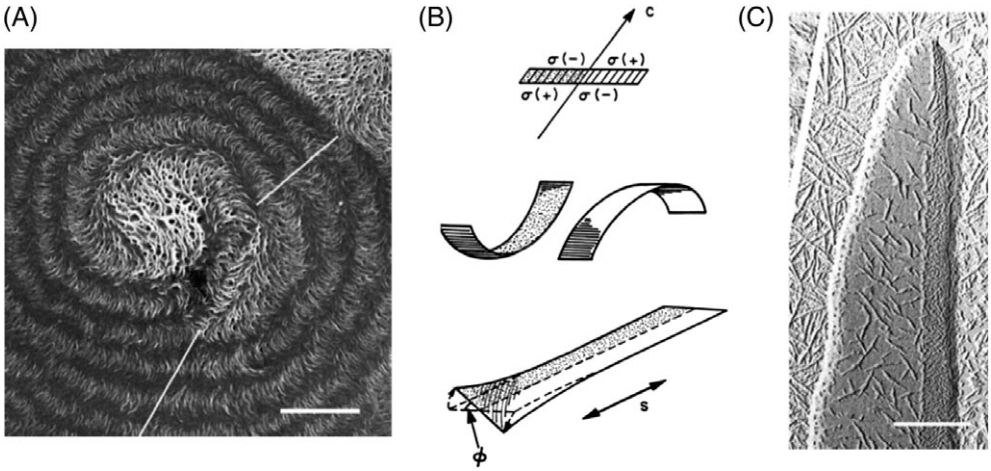

FIGURE 6 A, Surface pattern observed by SEM of a PE spherulite grown in the melt. The concentric bands are because of twisted lamellae reaching the surface. In the lower right and upper left parts, the lamellae have right-handed and left-handed twists, respectively. Scale bar: 10 μm. B, Proposed model by Keith and Padden to illustrate the unbalanced surface stresses [$\sigma(+)$ and $\sigma(-)$] caused by stem tilts in the ac plane normal to the growth direction, which further lead to bending of the half lamellae and twisting of the lamellae. C, PE decoration pattern on a flat-on single crystal of PE reveals two growth sectors with different folded surface layers. Scale bar: 1 μm.
Panel (A) adapted from Ref. [29] with permission; copyright 2005 Elsevier Ltd. Panel (B) adapted from Ref. [30] with permission; copyright 1984 Elsevier ltd. panel (C) adapted from Ref. [31] with permission; copyright 1989 American Chemical Society

Most evidence to support the existence of such stress is based on crystal morphology observations, which are frequently associated with crystal bending, scrolling and twisting of a single lamellar crystal. Chrysotile, which is a layered silicate, provides a clear example of curved crystal structures from nonpolymeric materials. This crystal structure is made of two different sheets connected by covalent bonds: A network of linked SiO_4 tetrahedra forms one sheet and a brucite type octahedral layer forms the other sheet. These two sheets possess different lattice parameters in their contact planes. As a result, the whole layer is curved and ultimately scrolled, with the "tighter" sheet inside to reduce surface stress.

The direct consequences of unbalanced surface stresses on crystal growth and morphology are bending, scrolling and twisting in lamellar crystals, although such morphological observations are not necessarily caused by unbalanced surface stresses. One most clear and certain illustration is perhaps the concentric extinction bands in polymer spherulites observed in PLM. Attempts to understand the crystallographic relationships in crystalline spherulites and their formation mechanism can be traced back to over half a century ago. However, it was only in the early 1950s, after the recognition of chain folding in polymer lamellar crystals and of the fact that spherulites are made of radial lamellae with a constant thickness, that the concentric extinction rings were associated with cooperative lamellar twisting. In later years, such a deduction was experimentally confirmed using scanning electron microscopy (Figure 6A).

The origin of lamellar twisting has been debated for many years. In 1984, Keith and Padden invoked the concept of surface stresses to explain the lamellar twisting phenomenon. They pointed out that when unbalanced surface stresses exist on the opposite sides of the half-lamellar crystals, lamellar twisting would take places, as illustrated in Figure 6B. For PE, the chain stems are tilted toward the a axis *in the ac plane* of the lamellar crystals, which is perpendicular to the spherulite growth direction (Figure 7B). This tilting creates an acute angle and an obtuse angle at the opposite ends of the stem on opposite lamellar surfaces. It was suggested that the folding conformations at these acute and obtuse angled locations differ, thus create different degrees of overcrowding and generate different surface stresses, which further results in the scrolling of half lamellae in opposite directions. One of the two half lamellae prefers to scroll down whereas the other would scroll up if they were independent. But since these two half lamellae are connected together within a single crystal, the opposite scrolling of the half lamellae leads to a whole lamellar twisting to relieve the opposite scrolling tendencies. The PE decoration technique provided clear evidence that the opposite half lamellae showed very different folded surface topologies (Figure 6C). Detailed explanations can be found in our most recent publication.[32]

The observation of concentric extinction bands, either regular or irregular, is frequent in a number of polymer spherulites, which indicate that lamellar twisting single crystals have been observed (Figure 7A).[33] Others typical examples are some biopolymers (Figure 7B)[34] and poly(hydroxyvalerate) (Figure 7C).[35] Many diverse hypotheses have been proposed to explain this lamellar twisting phenomenon, as recently reviewed by Bart Kahr et al.[36] Individual lamellae do indeed twist, as illustrated in Figures 7A,B.[15,16] The origin of the twist must lie in the structure of individual lamellae and frequently in their fold surfaces that are structurally different from the crystalline core.[32] The asymmetry of the structure in opposite fold surfaces as postulated for PE may result from different folding conformations, chemical compositions, and/or packing densities or of course from any combination of such differences could be the cause of lamellar twisting.

Lamellar twist is a chiral process––lamellar twist may be right- or left-handed in PE spherulites, as a result of opposite (clockwise or anticlockwise) chain tilt in the lamella (Figure 6A). The lamellar twist is not a manifestation of the molecular and helical conformational chirality, as illustrated with spherulites of poly [(*R*)-3-hydroxyvalerate] (Figure 7c).[35] This polyester possesses a chiral helical conformation. The helices pack in a *near*-tetragonal unit cell. Since the unit cell

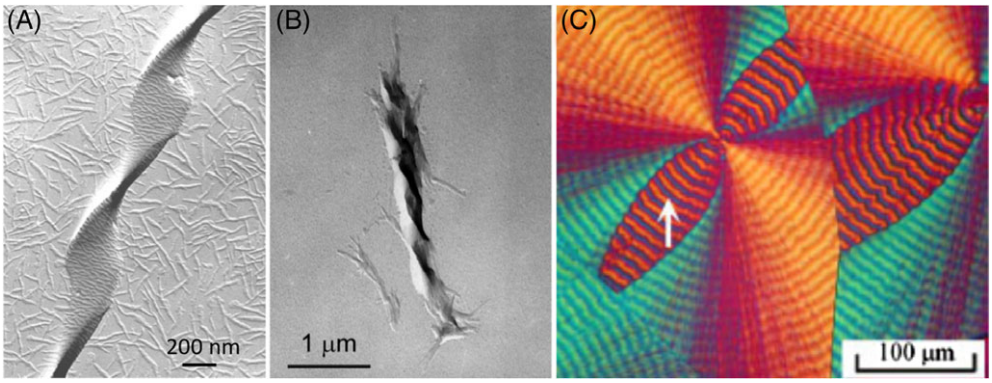

FIGURE 7 Examples of twisted morphology in polymer crystals. A, Twisted single crystal of a main-chain chiral polyester with PE decoration. B, Twisted crystal of *Bombyx mori* L. silk fibroin crystallized from an aqueous solution of LiBr by slow dialysis against water. C, PLM image of poly [(*R*)-3-hydroxyvalerate isothermally crystallized at 70°C. the white arrow indicates one of the eye-like regions with alternating positive and negative birefringent bands and opposite lamellar twist sense to the neighbor regions.
Panel (A) adapted from Ref. [33] with permission; copyright 1999 American chemical society. Panel (B) adapted from Ref. [34] with permission; copyright 1982 Elsevier ltd. Panel (C) adapted from Ref. [35] with permission; copyright 2009 American Chemical Society

exhibits *near*-symmetry, the growth rates along the *a* and *b* axes are nearly identical. The spherulites thus can grow along two possible radial directions (either along the *a*- or the *b*-axes, Figure 7C) to form different sectors. The lamellar twist sense is found to be different in these sectors. As a result, within one spherulite of a chiral polymer, the two opposite lamellar twist senses coexist, depending on the radial growth direction. The lamellar twist sense is dictated by the surface stresses and structure, but certainly not by the chirality of the constituent chains and helices.

If the unbalanced surface stress occurs at a whole single lamellar crystal (not half lamellae), as is the case in the absence of two-fold or two-fold screw axis along the growth direction, it leads to lamellar scrolling. One of the clearest experimental evidence was reported recently in a study on two specially designed triblock terpolymers with a middle crystalline block and two amorphous, immiscible end-blocks: polystyrene-*block*-poly(ethylene oxide)-*block*-poly(1-butene oxide) (PS-*b*-PEO-*b*-PBO) and polystyrene-*block*-poly(ethylene oxide)-*block*-polydimethylsiloxane (PS-*b*-PEO-*b*-PDMS). The design is to purposely synthesize different molecular weights (and thus, volumes) on the opposite sides of the two phase separated amorphous blocks, and make the middle PEO blocks to crystallize in to single crystal lamellae, unbalanced surface stress is thus generated. As shown in Figure 8, the schematic cartoon illustrates the idea of possible mechanism in generating scrolled single crystals, which qualitatively matches the experimental observations of large scrolled single crystals of PS-*b*-PEO-*b*-PBO grown in dilute solution using the self-seeding procedure at low supercooling. The scrolling direction is along the (120) planes. Within these single crystals, three layers of distinct chemical compositions can be identified from the edges of the single crystals after RuO_4 staining under high-resolution TEM utilizing high tilting angles, suggesting that the two microphase layers of the amorphous PS and PBO end-blocks are segregated on the opposite sides of PEO single crystals. Although both blocks possess identical tethering density on the surfaces of PEO crystals, their reduced tethering densities are different because of different molecular weights (volumes), which results in dissimilar surface crowdedness on the opposite sides of the crystals. The unbalanced surface stress is thus generated and the whole lamellar single crystal scrolls.

A morphologically similar curved structure has been found in a form of concentric lamellae in self-assembling block copolymers (Figure 9). Again, the formation of this type of curved lamellar structure results from the different size of the polymeric blocks. Therefore,

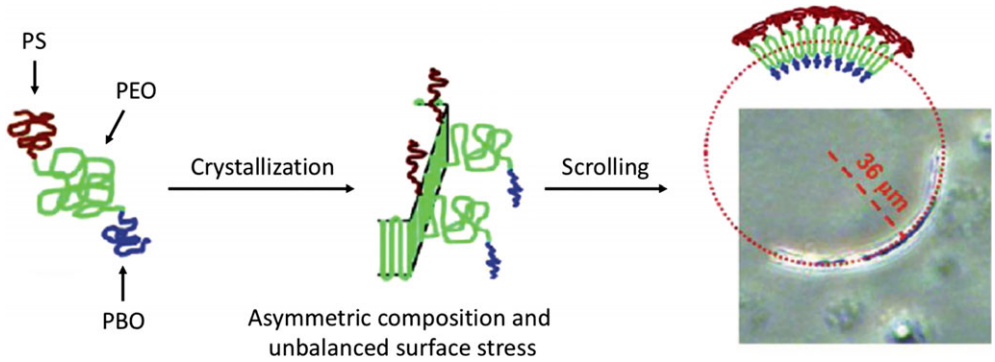

FIGURE 8 Cartoon illustration of the formation of a scrolled single crystal from a triblock copolymer PS-*b*-PEO-*b*-PBO with a crystalline middle block. After crystallization of the middle block, the resulting single crystals are scrolled because of the different molecular weights of two end blocks.
Adapted from Ref. [37] with permission; copyright 2011 American Chemical Society

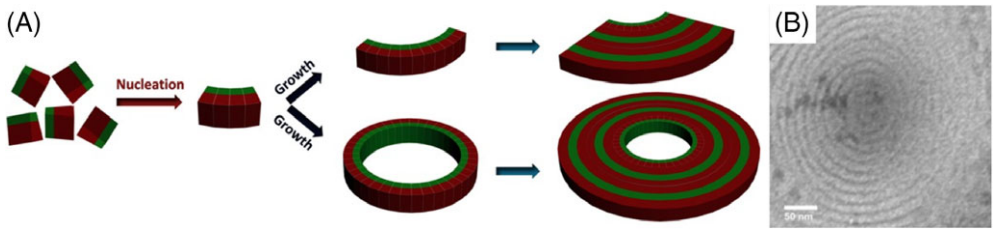

FIGURE 9 (A) TEM image and (B) proposed formation mechanism of the concentric lamellae from a special block copolymer. Scale bar: 50 nm. Adapted with permission from Ref. [38]; copyright 2016 John Wiley and Sons

a truncated-wedge-like molecular shape as nuclei induces morphological curvature during self- assembly, and forms curved and concentric lamellae. This result also confirms the critical role of unbalanced surface grafting density to influence the bending of a lamellar structure.

In two specific cases, the molecular origin of asymmetric surface stresses inducing scrolling could be associated with the chemical constitution of the folds in chain-folded polymer crystals and the different fold volume in the opposite sides of the lamella. In the γ form crystals of PVDF (Figure 10A),[39,40] the folds have different numbers of CH_2 and CF_2 units (eg, 4 and 3 vs 3 and 4, respectively): the volume difference is only 10 $Å^3$. In nylon 66 single crystals formed in glycerin (Figure 10B)[41] folds made in the amide and acid parts of the repeat unit differ by the number of CH_2 units (in this case, 6 vs 4, respectively). In the scrolled crystals of the form III of poly(butane-1) crystallized in amyl acetate (Figure 10C),[42] different fold conformations might be involved. Recognition of scrolled crystals as a building entity of polymer spherulites has been a significant advance in polymer morphology. In particular, it helped analyze the complex structure of unusual, negatively birefringent spherulites of even-even spherulites first observed in 1949. These spherulites are built-up with a frame of radiating scrolled crystals and an in-filling, additional growth of radial lamellae.[43] Note that the origin of scrolling resides in the lamella or fold structure(s). Two-dimensional (2D) scrolled polymer lamellae can also be observed, for example in aluminoxate nanotubes, but in that case the lamellar geometry reflects the confined growth.

Recently, Li et al. reported the formation of "crystalsomes" in solution.[45] They took advantage of surfactant micelles to confine the crystalline tails of poly(L-lactic acid; PLLA), and the crystallization resulted in scrolled and twisted lamellar crystals on the 2D scrolled micellar inner-surfaces (Figure 11). Note that all scrolled and twisted lamellar crystals do not possess 3D translational symmetry. The neighboring stems in the crystals are not strictly parallel to each other. Therefore, they are not, strictly speaking, in the class of traditionally defined crystals. However, the tilt or splay angle is very small. Only the morphology helps establish it and helps analyze the underlying molecular/structural origin.

4 | FLOW-INDUCED CRYSTALLIZATION OF POLYMER

Flow-induced crystallization of polymers is a process generally far away from equilibrium in nature. This process is commonly associated with polymer processing such as fiber spinning, film blowing, injection molding, and others. Compared with crystallization under quiescent conditions, imposing flow during crystallization is able to greatly increase crystallization rates by several orders of magnitude. Sometimes, flow-induced crystallization may also lead to new crystal structures and morphologies such as elongated crystal spherulites and the shish-kebab crystals. Practically, flow-induced crystallization thus not only plays an important role in tuning the stability and efficiency of

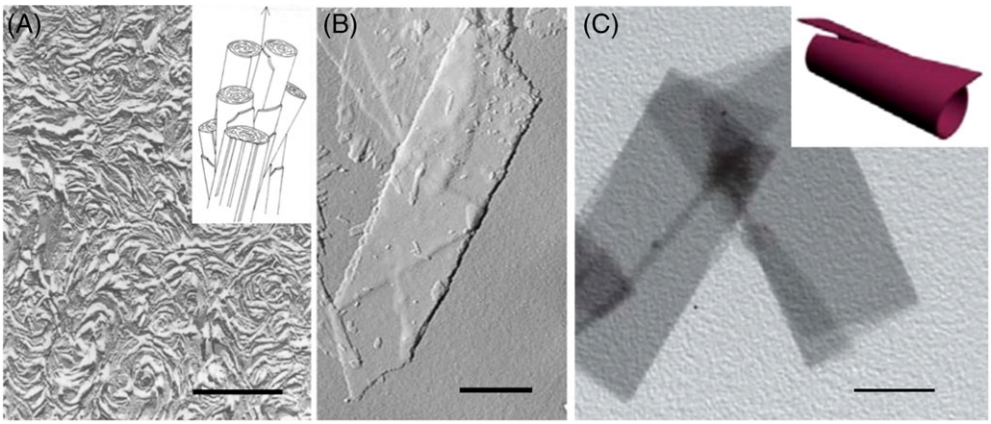

FIGURE 10 A, Scrolled lamellae morphology in γ-PVDF spherulites, with the initial drawing of Vaughan to illustrate the scrolled lamellae revealed by etching as the inset. Scale bar: 1 μm. B, Scrolled crystal of nylon-66 formed at 172°C in a dilute solution of glycerin. It became flat when deposited on the substrate carbon film. Scale bar: 500 nm. C, Form III single crystals of poly(butane-1) exhitits crolled single crystals grown in in amyl acetate. The inset indicates single crystal morphology in solution. Scale bar: 2 μm.
Panel (A) adapted from Ref. [39] with permission; copyright 1993 Chapman & Hall. Panel (B) adapted from Ref. [41] with permission; copyright 2004 John Wiley and Sons. Panel (C) adapted from Ref. [44] with permission

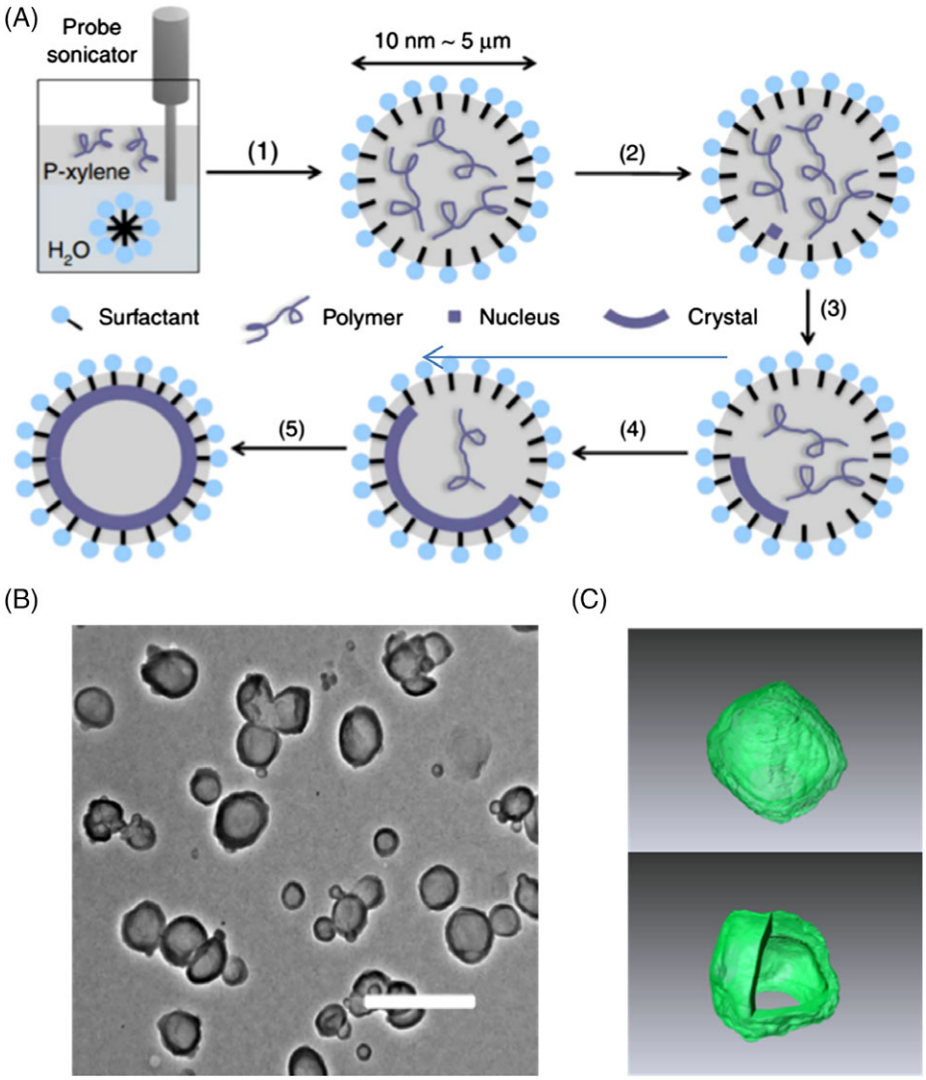

FIGURE 11 A, Schematic illustration of the formation mechanism of surfactant micelles with PLLA tails. These PLLA tails can be crystallized on the curved micellar inner-surfaces to from 2D curved single crystals. B, TEM image showing the micelles with curved 2D PLLA crystals as the shell. Scale bar: 1 μm. C, Reconstructed models of the crystalsomes from 3D tomographic technique.
Adapted from Ref. [45] with permission; copyright 2016 Springer Nature Limited

polymer processing, but also controls the properties of polymeric products.[46,47] In making further understanding of flow-induced crystallization, advanced experimental techniques such as synchrotron radiation facility and computer simulation have made great progresses toward this aspect.[48,49] Nevertheless, the establishment of molecular and supramolecular behaviors during flow-induced crystallization that correlates with such fast crystallization kinetics is still awaited.

Historically, the general thermodynamic understanding of flow-induced crystallization in polymers has been associated with the entropic reduction of chain molecules under flow or stretch.[50,51] The decreased entropy in stretching melts result in an increasing of the melting temperature, and thus, enlarges supercooling during the crystallization to make crystallization kinetics faster. In the cases of low flow rates in the melts, or in oriented solution crystallization, such as the coil-stretch transition to explain the formation of the shish-kebab crystal morphology,[52] this simple explanation may be suitable. However, fast flow rates under shear or elongation processes, this simple thermodynamic explanation is not sufficient to account for such fast crystallization rates observed experimentally. Furthermore, this understanding is based on the consideration of flow effects to cause conformational changes at the global chain length scale, which takes the coarse-grained approach similar to that adopted in rheological studies. However, detailed descriptions of flow-induced polymer crystallization also require detailed molecular structures for crystal packing. In this section, we will review recent experimental observations in this field and hopefully, to provide some lightening for understanding of flow-induced polymer crystallization.[53,54]

Traditional understanding for shish-kebab formation in solution is that at a specified flow field, chains longer than a critical length are stretched whereas other short chains remain in their coil state. Correspondingly, the stretched long chains form the shish and the coiled short chains grow on the shish surface to form kebabs.[55] The description is reasonable to explain the experimental observations of shish-kebab formation. Later, this description has also been extended to explain the shish-kebab formation in polymer melts during flow-induced crystallization. However, this extension is questionable since

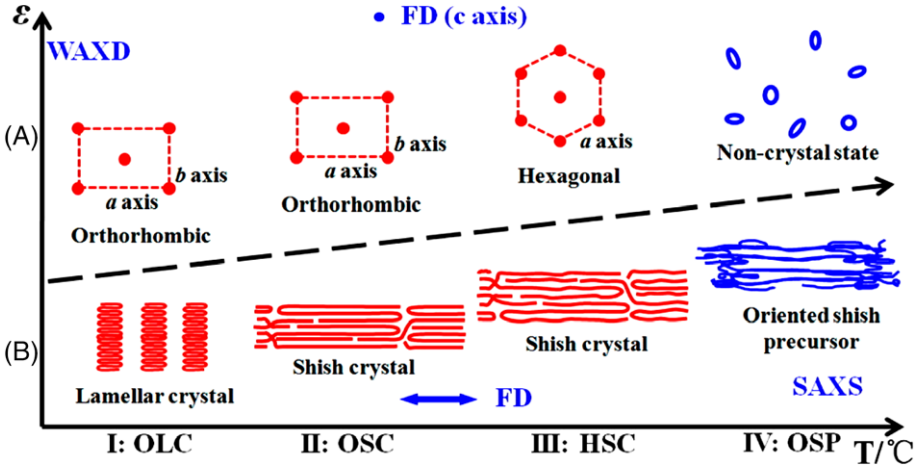

FIGURE 12 Schematic of the morphologies and structures of four regions in the strain-temperature space deduced from both WAXS and SAXS: An orthorhombic lamellar crystal (OLC), an orthorhombic shish crystal (OSC), a hexagonal shish crystal (HSC), and an oriented shish precursor (OSP) structure.
Reproduced with permission from Ref. [67]. Copyright 2014 American Chemical Society

in polymer melts, there is no macroscopic large-scale shish-kebab formations as in the polymer solutions. Vast majority reports are those observations of micro-shish-kebabs.[55,56]

Experimentally, with a combination of extensional rheometer and in-situ synchrotron radiation small/wide angle X-ray scattering (SAXS/WAXS), Yan et al. demonstrated that the critical macroscopic strain for micro-shish formation should be much smaller than that required to fully stretch polymer chains.[57] They further applied in-situ small angle neutron scattering measurements on lightly cross-linked PE samples and showed that a molecular stretch ratio of about 1.3 is sufficient to induce the formation of micro-shish structures.[58]

de Gennes' proposed a coil-stretch theory in dilute polymer solution, where polymer chains behave as Zimm chains.[59] Below the critical flow rate of this coil-stretch transition, the screening effect makes polymer chains and solvent molecules around move together, while above the critical flow rate, polymer chains cannot move with the solvent molecules anymore and thus the abrupt coil-stretch transition takes place. While in entangled polymer melts, the hydrodynamic interaction is negligible because of the identical mobility of all molecules and polymers behave as Rouse chains, where the essential physical ingredient for coil-stretch transition does not exist. Therefore, the coil-stretch transition cannot account for the micro-shish formation in polymer melts. As discussed later, starting with entangled networks without the presence of coil-stretch transition, it is still possible to generate shish by simply considering the nucleation barriers for nuclei with different structures or morphologies. Note that under real experimental conditions, the formation of micro-shish may proceed via different approaches, such as ghost nucleation,[60] phase separation,[61,62] shear banding,[63] etc.,[64–66] where structural and rheological heterogeneities or multi-stage structural evolutions play an important role.

Furthermore, different crystalline modifications and morphologies have been widely observed in flow-induced crystallization in polymers. Figure 12 shows common structures of flow-induced crystallization of PE as an example. Three different nuclei and their corresponding crystal structures, including an orthorhombic crystal in which both lamellar and shish forms can be observed at different flow rates, a hexagonal shish crystal, and a noncrystalline shish (NCS), have been observed at different temperatures.[67]

Similar to that observed in PE, different crystal modifications and morphologies have also been observed in flow-induced crystallization of isotactic polypropylene (it-PP) and poly(1-butene) (PB-1). Figure 13A-C present the nonequilibrium phase diagrams of PE,[68] it-PP[69] and PB-1,[70] respectively. For it-PP, in addition to the common α form crystals, NCS and β form crystals are also observed in high strain rate and high temperature region, whereas form III of PB-1 can be induced at high flow rates, which is actually metastable with a typical life time of tens of microseconds. In solution crystallization, this form III can possess a long stable live-time. The occurrence of new crystal modification and morphologies different from those at quiescent conditions suggests that flow not only reduces the entropy of initial polymer melts, but also alters the free energy nucleation barriers of crystalline states.

Inspired by above experimental observations, Liu et al.[67] developed a model incorporating both flow-induced entropic reduction of the melt and free energy nucleation barrier change of crystal nucleus. This correlates the onset temperature of crystallization with stretch ratio with the following equation:

$$\frac{1}{T_c(\alpha_i)} = \frac{1}{T_c(1)} - \frac{vk(\alpha_i^2 + 2/\alpha_i - 3)}{2\Delta H(1 - 4\sigma_e/\Delta H l^*)} \quad (3)$$

where $T_c(1)$ and $T_c(\alpha_i)$ are the crystallization temperatures at stretch ratios of 1 and α_i, respectively, l^* the critical nuclei thickness, v the network-chain density.[71] The term $vk(\alpha_i^2 + 2/\alpha_i - 3)/2$ represents the entropic reduction of the polymer melt, whereas $\Delta H(1 - 4\sigma_e/\Delta H l^*)$ is deduced from the Thomas-Gibbs equation to account for the structure and morphology of nuclei. This model incorporates almost all the important factors that affect the free energy changes from an initial melt (α_i) to a final crystal (σ_e, ΔH, and l^*), which is therefore capable to account for not only the enhanced nucleation rates but also the new crystal modifications and morphologies. With this model, the critical nuclei thicknesses l^* for OLC, OSC, and HSC are estimated to be in the orders of 10, 100,

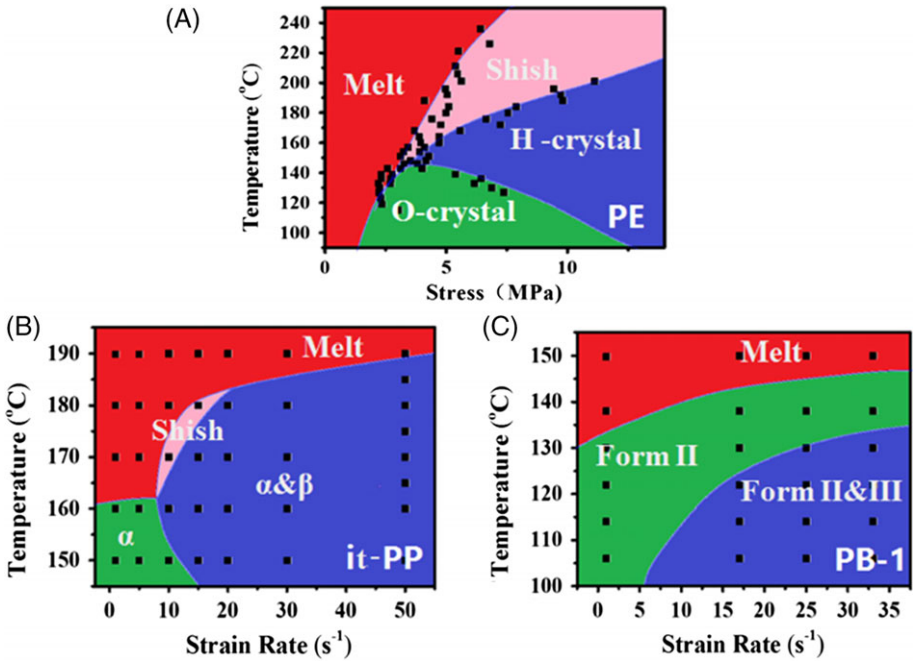

FIGURE 13 Nonequilibrium phase diagram of (A) PE (H = hexagonal; O = orthorhombic), (B) it-PP, and (C) PB-1 in flow-temperature space. α and β are α and β crystals, respectively. (B) Relative content of β crystals in strain rate-temperature space.
Panel (A) adapted with permission from Ref. [68]; copyright 2016 springer nature limited. Panel (B) adapted with permission from Ref. [69]; copyright 2016 John Wiley and Sons. Panel (C) adapted with permission from Ref. [70]; copyright 2017 Royal Society of Chemistry

and 500 nm, respectively, suggesting a natural transition from lamellar to shish nuclei.

Although this model can account for most observations in flow-induced crystallization experiments, it is still a simplified two-phase phenomenological model based on classical nucleation theory, which is a one-step process and does not consider intermediate orders. Although the existence of preorder or precursor prior to crystallization at quiescent conditions is still a debating issue, it seems being accepted that preorder can emerge in flow-induced crystallization.[72–75] As the flow-temperature phase diagrams in Figure 13 shows, NCS structure occurs in flow-induced crystallization of PE and *it*-PP, which serves as the intermediate order to assist crystal nucleation. Actually with cyclic extension experiments, the shish structure in PE has been demonstrated to be stable enough, which can undergo mutual transformation to either the melt or the hexagonal phase.[68]

Even in the very early period of crystallization prior to detecting any ordered structure, flow-induced crystallization may undergo the stage of precursor, as often found in the studies about the memory effect.[76–78] A recent example is presented in Figure 14, in which it-PP samples were sheared by pulling glass fibers at different high temperatures and then cooled down to 138°C for isothermal crystallization. With synchrotron radiation scanning X-ray micro-diffraction (SR-μSXRD), Su et al. mapped the crystallinity distribution around the glass fibers at the shearing and the isothermal crystallization temperatures.[72] Before cooling down to 138°C, flow-induced crystallization already occurred in it-PP samples sheared at 160 and 165°C, whereas crystal diffraction could be observed only after cooling down to 138°C for samples sheared at 170 and 175°C. Interestingly, as evidenced by the cylindrical crystallites around the glass fibers, shear at 175°C did promote crystallization, however, it still took an induction time of about 230 seconds for crystallization to occur after cooling down to 138°C. If crystal nuclei already formed just after shearing, we would see a direct growth of crystals without any induction time. Note that after cessation of fiber shear, it took more than 10 minutes to complete the SR-μSXRD measurement at 175°C and the cooling process to 138°C, which was far longer than the terminal relaxation time τ_d of it-PP chains under the experimental condition (0.65 seconds at 175°C), indicating that the shear-induced ordered structure was not simply because of chain orientation. The existence of induction time can exclude the argument on detection sensitivity of

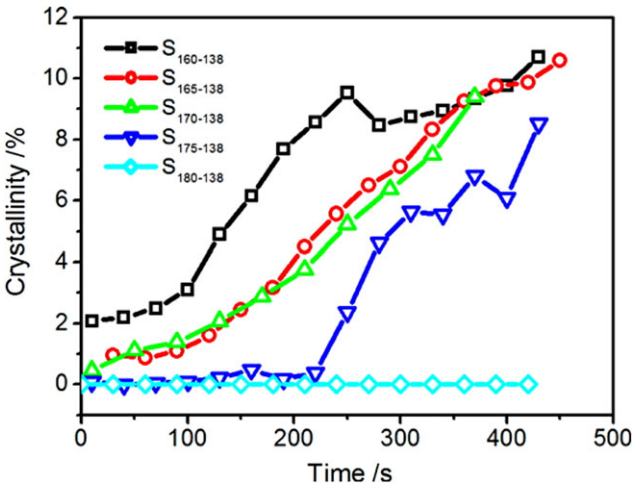

FIGURE 14 Evolution of crystallinity during isothermal crystallization at 138°C of samples after shear at different temperatures.
Reproduced with permission from Ref. [72]; copyright 2014 American Chemical Society

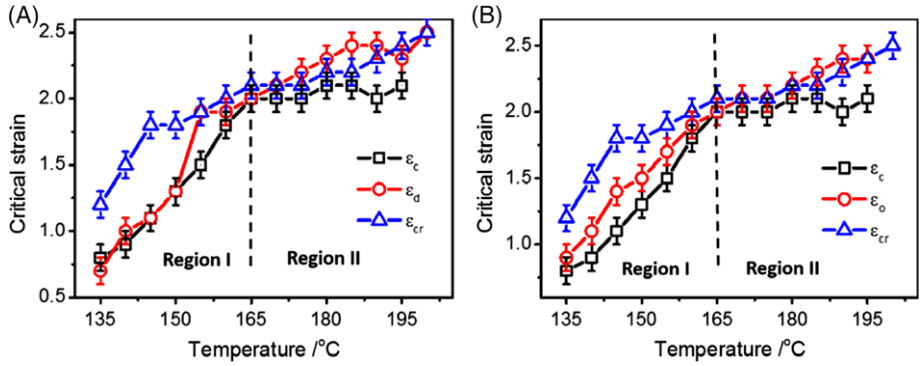

FIGURE 15 Summary of transition strains (A) ε_c, ε_d, and ε_{cr} and (B) ε_c, ε_o, and ε_{cr} during extension at different temperatures.
Reproduced with permission from Ref. [82]; copyright 2017 American Chemical Society

SR-μSXRD and suggests that shearing indeed induces noncrystalline precursors involving multi-chain interactions with longer lifetimes than the terminal time τ_d.

For polymer crystals, the unique molecular aspect is the ordered segmental conformation, such as the trans-segments in PE and the 3/1 helices in *it*-PP. The transformation from flexible polymer chains into conformationally rigid, ordered crystalline segments is the most critical step for polymer crystallization. As predicted by theory,[79] imposing flow can promote the formation of helices through coil-helix transition because of entropic reduction, which may further organize into the precursors observed in flow-induced crystallization.[80,81] Following this line, several groups have applied spectroscopic methods, like Raman and infrared (IR) spectroscopy, to investigate the flow-induced conformational ordering. Figure 15 presents a recent study by using in-situ IR and SAXS/WAXS measurements on lightly cross-linked it-PP samples during extension at different temperatures.[82] The absorption bands at 998 and 841 cm^{-1} in IR spectra were employed to track coil-helical transition and possible orientational ordering, respectively, whereas SAXS and WAXS profiles were recorded to detect density fluctuation and crystallization, respectively.

Through following emergences of specific structural signals during extension at different temperatures, the critical strains for level-up of helical content (ε_c), density fluctuation (ε_d), orientational order (ε_o), and crystallization (ε_{cr}) were extracted and plotted in Figure 15 against temperature. At below 165°C (melting temperature of it-PP), ε_c and ε_d were found identical, which were obviously smaller than ε_{cr}, indicating that preordering coupled of conformational order and density fluctuation occurs prior to the onset of crystallization. As the band at 841 cm^{-1} was corresponding to the presence of long helices that were capable to induce nematic ordering ε_c, $\varepsilon_d < \varepsilon_o < \varepsilon_{cr}$ also suggested isotropic-nematic transition might take place after density fluctuation but prior to crystallization.

Based on the above experimental observations, a schematic multi-scale ordering process for flow-induced crystallization was proposed by Su et al.[82] (see Figure 16), which showed a sequential ordering process as the conformational order-density fluctuation-preordering-crystallization. Imposing flow on entangled polymer melts leads to intra-chain conformational ordering or coil-helical transition, which has been demonstrated by both theoretical predictions[79] and experimental observations mainly from in-situ spectroscopic methods.[82–85] Flow-induced coil-helical transition has also been confirmed by molecular dynamic computer simulations.[86] As flow proceeds, the increase of helical content eventually brings interactions among helices, which present as either density fluctuation or preordering. The occurrence of NCS prior to crystallization has been widely observed with simultaneously synchrotron radiation SAXS/WAXS measurements, where the streak signal in SAXS demonstrates the density contrast between shish and the matrix melt. While the presence of preorder before the onset of crystallization is based on theoretical suggestion rather than direct experimental evidence. Nevertheless, the steak signal in SAXS is always highly oriented, which suggests parallel orientation of helical segments inside shish and may indirectly support the occurrence of preordering.

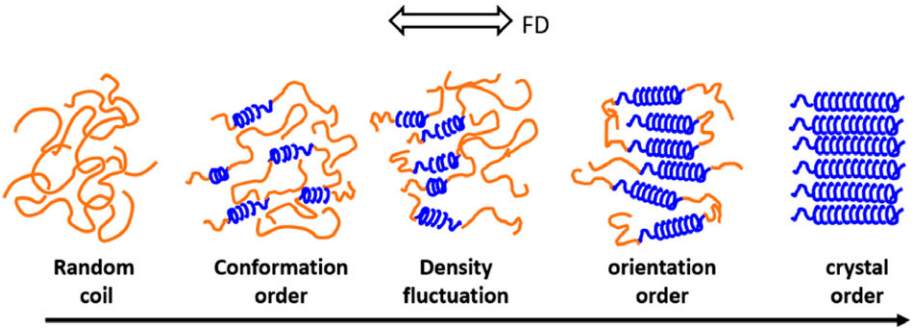

FIGURE 16 Schematic illustration of FIC proceeding via a multi-scale ordering process. The extensional flow direction is horizontal, as indicated by the double-headed arrow.
Reproduced with permission from Ref. [82]; copyright 2017 American Chemical Society

Comparing with quiescent crystallization, flow-induced crystallization behaves fundamentally different, which mainly comes from flow-induced conformational ordering or coil-helical transition. The conformational ordering is a critical step in polymer crystallization, which cost large entropic penalty. If flow promotes coil-helical transition and circumvent the entropic penalty, flow-induced crystallization may proceed via different kinetic pathways from that at quiescent conditions. In current models for flow-induced crystallization, the same one-step pathway is assumed in crystallization under both quiescent and flow conditions, whereas the entropic reduction of melt and the energy change of nuclei induced by flow are incorporated to shift melting point or crystallization temperature. Evidently, as shown in Figure 16, the molecular mechanism for flow-induced crystallization has to consider the different kinetic pathways under various flow condition.

5 | SUPRAMOLECULAR CRYSTALLIZATION OF POLYMERS

Traditional studies on polymer crystallization involve the ordered arrangements of polymer segments into crystalline lattices. Conversely, the past few decades have witnessed the development of an inter-discipline area, termed "supramolecular crystallization," which combines polymers with supramolecular chemistry.[87] In a typical supramolecular crystallization, polymers first self-assemble into nanometer-sized molecular/supramolecular "motifs" that can further pack into various supralattices with long-range order, thus forming so-called "supramolecular crystals." Distinct from the well-documented polymer crystals, whose motifs are identical combinations of atoms or polymer segments, the motifs of supramolecular crystals are assembled clusters, which typically contain a much larger number of atoms. Motifs in common polymer crystals repeat themselves with long-range positional, bond-orientational, and molecular orientational orders; whereas in supramolecular crystals, supramolecular motifs only possess long-range positional and orientational order at the length scale relevant to the size of the motifs. In other words, within each of the building block, atomic precision in positional, bond-orientational, and molecular orientational orders now should be changed to topological shape-orientational orders.

Probably the most famous example of polymer supramolecular crystallization is the microphase separation of block copolymers.[88,89] Driven by the chemical immiscibility of different polymer chains, block copolymers can self-assemble into ordered structures with feature sizes of typically tens of nanometers. The formation of such ordered structures can be experimentally investigated by the developed crystallographic techniques, such as X-ray scattering/diffraction methods.[88] It should be noted that the concept of supramolecular crystallization can also be extended to ordered structure formation in other systems at larger length scales. For examples, in colloidal crystals, parameters of supralattices are generally in the micrometer scale, depending on the size of the colloidal motifs.[90]

Supramolecular crystallization of block copolymers has been extensively studied during the past years. In common diblock copolymers, depending on the relative volume fractions of each block, a set of ordered structures, such as alternating lamellae (LAM), double gyroids (DG), hexagonally packed cylinders (HEX), and spheres in body-center cubic (BCC) lattices, are generally observed in the bulk.[88] When confined in thin films on a substrate, similar structures have also been identified with tunable lattice alignment directions in respect to the substrate.[91] This unique behavior of block copolymers has led to different potential applications, such as in the templated synthesis of nanomaterials and in the so-called block copolymer lithography.[92] The latter is widely believed as a promising alternative approach to complement the current photolithography technique for the fabrication of ordered structures at sub-10 nm scales. To enhance the thermodynamic driving force for phase separation between different polymer blocks, recently, a series of high-χ polymers with low degree of polymerization have been reported to self-assemble into supralattices with sub-10 nm feature sizes.[93]

Interestingly, with the help of advanced organic synthesis, some monodispersed block copolymers composed of chemically bonded oligomers have been prepared.[94] The ideal monodispersity of such precise macromolecules could also result in nanostructures with high uniformity and thus generate in high orders.[95] Domain sizes of self-assembled structures of block copolymers are determined by the size or molecular weight of the compositional blocks. To achieve smaller feature sizes, our group has proposed a different approach other than lowering the molecular weights. We selected a group of molecules with 3D conformation, shape rigidity, and nanometer size, termed molecular nanoparticles (MNPs).[96] We reason that by replacing a flexible polymeric block by these nano-sized MNPs, the resulting self-assembled supramolecular structures should possess feature sizes similar to the building blocks. Following this idea of molecular design, we have demonstrated several types of novel macromolecules, such as giant surfactants (MNPs tethered with polymer chains),[97–99] shape amphiphiles (conjugates of MNPs through short linkers),[100,101] and giant polyhedra (nano-sized conjugates of MNPs with rigid shaped linkers),[102] as articulated in our recent Perspective Paper.[96] So far, widely used MNPs are derivatives of polyhedral oligomeric silsesquioxanes (POSS)[103–107] and [60]fullerenes (C_{60}).[108,109]

In general, this novel type of macromolecules constructed from MNPs, termed as "giant molecules," show interesting supramolecular crystallization behavior in the bulk and in thin film confinement. For example, in a prototype giant surfactant composed of a hydrophilic POSS head and a hydrophobic PS tail, we observed formation of several different ordered structures, which were similar to diblock copolymers but had sub-10-nm feature sizes and unusually high order.[97] By increasing the length of the PS tail and thus its volume fraction, all four common structures such as LAM, DG, HEX, and BCC can be obtained (Figure 17). Also, facilitated by the modular and efficient synthetic methods based on "click" reactions,[110] the giant surfactant system offered an unprecedented platform to tune their macromolecular topology and study the topology-induced effects on self-assembled nanostructures.[111] For example, even starting from the same precursors, by applying several steps of "click" reactions, the numbers of POSS heads and PS tails can be independently changed, resulting in so-called "multi-headed" giant surfactants and "multi-tailed" giant surfactants (Figure 17). Importantly, such molecular topology variations significantly alter the preferred conformation and

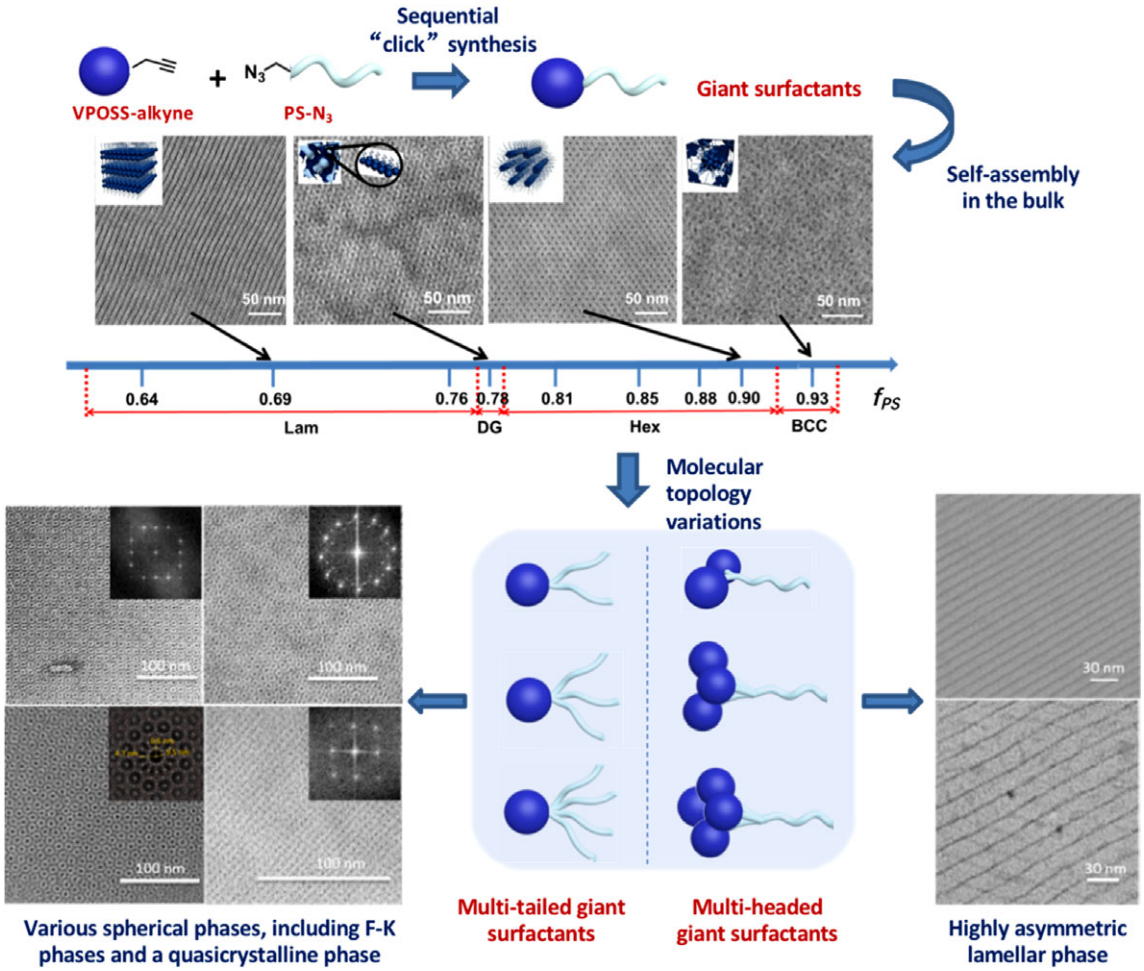

FIGURE 17 Summary of the study on POSS-based giant surfactants. Starting from "clickable" molecular building blocks, a modular "click"-type synthetic strategy can prepare a series of giant surfactants with tunable molecular topology, which further leads to rich self-assembly behaviors in the bulk.
Adapted from Refs. [97–99] with permission; copyright 2013 National Academy of Sciences copyright, 2016 National Academy of Sciences, and 2018 American Chemical Society

molecular shape, thus changing the structure of the supramolecular motifs and their further packing. This is clearly illustrated by the study on the so-called "topological isomers," which refer to a pair of macromolecules with an identical composition but different molecular topology.[111,112] In another example, multi-headed giant surfactants are found to form an unusual highly asymmetric LAM phase, as limited by the molecular shape and asymmetric junction curvature. The relative widths of alternating PS and POSS lamellae can reach over five in these samples (Figure 17).[99]

Perhaps the most interesting findings are the observation of some unconventional spherical phases in giant molecules, such as the Frank-Kasper phases and spherical quasicrystal phase.[113] These spherical phases were originally identified in metal alloys, in which the coordination number of certain atoms could be 12, 14, 15, or even 16. Recently, these structures have been revealed in soft matter,[114–116] especially in polymers.[117,118] Formation of such phases first requires the molecules to assemble into spherical motifs. Simply put, it means that the molecules should prefer a cone-like conformation to build up a spherical motif. In macromolecular science, Frank-Kasper and related quasicrystal phases have usually been seen in cone-shaped dendron molecules.[114,115,119] Only until very recently, a Frank-Kasper σ phase was found in block copolymers of specific compositions,[117] followed by other types of unconventional spherical phases[120] in the past few years.

Since self-assembly behavior of giant surfactants showed a high sensitivity on molecular topology, through topological engineering, we have revealed a molecular geometry-induced mechanism in the multi-tailed giant surfactants to explain the formation of unconventional Frank-Kasper and related quasicrystal phases vs the common BCC phase (Figure 17).[98] We found that several different spherical phases could be clearly identified in these multi-tailed giant surfactants with branched topology. Simply speaking, we believe that this molecular topology favors the cone-like conformation and expands the region of spherical motifs. Further packing of supramolecular motifs is altered as the volume fraction changes, because of a subtle balance between the interfacial energy and the stretching energy of the polymer tails.

6 | CONCLUSIONS AND OUTLOOK

To briefly conclude, after almost 70 years of intensive study, the field of polymer crystals and crystallization has achieved significant

progress to understand this phenomenon of critical scientific and practical importance. We have described a few selected topics in this field that still require more attention. Especially, theories on nucleation and crystal growth should be further developed with emphasis on the role of many metastable states along the process. This is a very difficult and challenging topic. Mean-field approaches only describe a system under thermodynamic equilibrium, whereas polymer crystallization is far away from this equilibrium. Furthermore, analytical equations to describe polymer crystallization based on this approach can hardly provide detailed trajectory of individual molecules during crystallization. Therefore, they can only be a representation of an average pathway for all the molecules. Yet, the transition pathway of each molecule is critically important for understanding metastable formation and transitions. The field of flow-induced crystallization of polymers, which is closely related to polymer processing and manufacturing, is the key to achieve polymer products with superior properties and performance. However, acceptable theoretical descriptions in this topic have to be waited for a long time. The crystal growth rates during flow deformation and elongation exhibit several orders of magnitude of enhancement, which breaks down the classical nucleation process. There are many complicated nonequilibrium processes that would affect the polymer crystallization. Further understanding is critically necessary not only for scientific purposes but also for practical applications. Lastly, by combining polymer crystallization with supramolecular chemistry, the emerging concept of supramolecular crystallization of polymers provides a means to take advantage of polymer self-assembly and create nanostructures with diverse symmetry and very low features sizes (sub-10 nm). Careful molecular design and precise synthesis of novel polymeric materials are still the key, which is certainly promoted by the development of controlled polymerization methods and highly efficient "click-type" reactions for postpolymerization functionalization. We believe that there are still a lot of opportunities for new discoveries in this old yet flourishing field.

ACKNOWLEDGMENTS

We gratefully acknowledge the financial support from the Pearl River Talents Scheme (No. 2016ZT06C322) and the Fundamental Research Funds for the Central Universities (No. 2017JQ001). S. Z. D. Cheng thanks the NSF grant (DMR-1408872) for support.

ORCID

Kan Yue https://orcid.org/0000-0003-1450-0279
Gengxin Liu https://orcid.org/0000-0002-2998-8572
Stephen Z. D. Cheng https://orcid.org/0000-0003-1448-0546

REFERENCES

[1] A. J. Lovinger, *Foreword in Phase Transitions in Polymers: The Role of Metastable States*. Elsevier. **2008**.
[2] H. D. Keith, F. J. Padden, *J. Polym. Sci.* **1959**, *39*, 101.
[3] H. D. Keith, F. J. Padden, *J. Polym. Sci.* **1959**, *39*, 123.
[4] R. Jaccodine, *Nature* **1955**, *176*, 305.
[5] P. H. Till, *J. Polym. Sci.* **1957**, *24*, 301.
[6] A. Keller, *The Philos. Mag.* **1957**, *2*, 1171.
[7] A. Keller, *Polymer* **1962**, *3*, 393.
[8] F. Khoury, E. Passaglia, *The Morphology of Crystalline Synthetic Polymers*, Plenum Press, New York **1976**.
[9] D. C. Bassett, *Principles of Polymer Morphology*, Cambridge University Press, Cambridge **1981**.
[10] F. C. Frank, M. Tosi, *Proc. R. Soc. London, Ser. A* **1961**, *263*, 323.
[11] K. Armitstead, G. Goldbeck-Wood, A. Keller, Polymer crystallization theories. in *Macromolecules: Synthesis, Order and Advanced Properties*, Berlin, Heidelberg, Springer **1992**, p. 219.
[12] B. Wunderlich, Crystal nucleation, growth, annealing. in *Macromolecular Physics*, Academic Press, New York **1976**.
[13] L. Zhu, B. R. Mimnaugh, Q. Ge, R. P. Quirk, S. Z. D. Cheng, E. L. Thomas, B. Lotz, B. S. Hsiao, F. Yeh, L. Liu, *Polymer* **2001**, *42*, 9121.
[14] Y.-L. Loo, R. A. Register, A. J. Ryan, *Macromolecules* **2002**, *35*, 2365.
[15] L. Zhu, S. Z. D. Cheng, B. H. Calhoun, Q. Ge, R. P. Quirk, E. L. Thomas, B. S. Hsiao, F. Yeh, B. Lotz, *J. Am. Chem. Soc.* **2000**, *122*, 5957.
[16] L. Zhu, S. Z. D. Cheng, P. Huang, Q. Ge, R. P. Quirk, E. L. Thomas, B. Lotz, B. S. Hsiao, F. Yeh, L. Liu, *Adv. Mater.* **2002**, *14*, 31.
[17] M. Volmer, M. Marder, *Zeitschrift für Physikalische Chemie* **1931**, *154*, 97.
[18] I. S. Gutzow, J. W. P. Schmelzer, *The Vitreous State: Thermodynamics, Structure, Rheology, and Crystallization*, Springer, Berlin, Heidelberg **2013**.
[19] R. L. Cormia, F. P. Price, D. Turnbull, *J. Chem. Phys.* **1962**, *37*, 1333.
[20] B. Vonnegut, *J. Colloid Sci.* **1948**, *3*, 563.
[21] M. V. Massa, J. L. Carvalho, K. Dalnoki-Veress, *Eur. Phys. J. E* **2003**, *12*, 111.
[22] M. V. Massa, K. Dalnoki-Veress, *Phys. Rev. Lett.* **2004**, *92*, 255509.
[23] S. Z. D. Cheng, B. Lotz, *Polymer* **2005**, *46*, 8662.
[24] M. A. Shcherbina, G. Ungar, *Polymer* **2006**, *47*, 5505.
[25] M. A. Shcherbina, G. Ungar, *Polymer* **2007**, *48*, 2087.
[26] T. Okihara, L. Cartier, G. O. R. Alberda Van Ekenstein, B. Lotza, *Polymer* **1999**, *40*, 1.
[27] S. Z. D. Cheng, B. Lotz, *Philos. Trans. A, Math., Phys. & Eng. Sci.* **2003**, *361*, 517.
[28] S. Z. Cheng, *Phase Transitions in Polymers: The Role of Metastable States*, Amsterdam: Elsevier, **2008**.
[29] B. Lotz, S. Z. D. Cheng, *Polymer* **2005**, *46*, 577.
[30] H. Keith, F. Padden Jr., *Polymer* **1984**, *25*, 28.
[31] H. Keith, F. Padden Jr., B. Lotz, J. Wittmann, *Macromolecules* **1989**, *22*, 2230.
[32] B. Lotz, T. Miyoshi, S. Z. D. Cheng, *Macromolecules* **2017**, *50*, 5995.
[33] C. Y. Li, D. Yan, S. Z. Cheng, F. Bai, T. He, L.-C. Chien, F. W. Harris, B. Lotz, *Macromolecules* **1999**, *32*, 524.
[34] B. Lotz, A. Gonthier-Vassal, A. Brack, J. Magoshi, *J. Mol. Biol.* **1982**, *156*, 345.
[35] H.-M. Ye, J. Xu, B.-H. Guo, T. Iwata, *Macromolecules* **2008**, *42*, 694.
[36] A. G. Shtukenberg, Y. O. Punin, A. Gujral, B. Kahr, *Angew. Chem. Int. Ed.* **2014**, *53*, 672.
[37] H. Xiong, C.-K. Chen, K. Lee, R. M. Van Horn, Z. Liu, B. Ren, R. P. Quirk, E. L. Thomas, B. Lotz, R.-M. Ho, W.-B. Zhang, S. Z. D. Cheng, *Macromolecules* **2011**, *44*, 7758.
[38] X. H. Dong, B. Ni, M. Huang, C. H. Hsu, R. Bai, W. B. Zhang, A. C. Shi, S. Z. Cheng, *Angew. Chem. Int. Ed.* **2016**, *55*, 2459.
[39] A. S. Vaughan, *J. Mater. Sci.* **1993**, *28*, 1805.
[40] B. Lotz, A. Thierry, S. Schneider, *Comptes Rendus de l'Academie des Sciences Series IIC Chemistry* **1998**, *1*, 609.
[41] W. Cai, C. Y. Li, L. Li, B. Lotz, M. Keating, D. Marks, *Adv. Mater.* **2004**, *16*, 600.
[42] V. F. Holland, R. L. Miller, *J. Appl. Phys.* **1964**, *35*, 3241.
[43] B. Lotz, S. Z. D. Cheng, C. Y. Li, *Macromolecules* **2018**, *51*, 5138.
[44] H.-J. Sun, University of Akron **2012**.
[45] W. Wang, H. Qi, T. Zhou, S. Mei, L. Han, T. Higuchi, H. Jinnai, C. Y. Li, *Nat. Commun.* **2016**, *7*, 10599.
[46] S.-G. Yang, Z. Zhang, D. Zhou, Y. Wang, J. Lei, L. Li, Z.-M. Li, *Macromolecules* **2015**, *48*, 5834.
[47] Y.-H. Chen, Y.-M. Mao, Z.-M. Li, B. S. Hsiao, *Macromolecules* **2010**, *43*, 6760.
[48] M. Okura, O. O. Mykhaylyk, A. J. Ryan, *Phys. Rev. Lett.* **2013**, *110*, 087801.

[49] O. O. Mykhaylyk, P. Chambon, R. S. Graham, J. P. A. Fairclough, P. D. Olmsted, A. J. Ryan, *Macromolecules* **2008**, *41*, 1901.
[50] P. J. Flory, *J. Chem. Phys.* **1947**, *15*, 397.
[51] P. J. Flory, *J. Chem. Phys.* **1947**, *15*, 684.
[52] A. Keller, H. Kolnaar, in *Flow Induced Orientation and Structure Formation*, Vol. 18, Processing of Polymers. VCH: New York **1997**.
[53] K. Cui, Z. Ma, N. Tian, F. Su, D. Liu, L. Li, *Chem. Rev.* **2018**, *118*, 1840.
[54] Z. Wang, Z. Ma, L. Li, *Macromolecules* **2016**, *49*, 1505.
[55] B. S. Hsiao, L. Yang, R. H. Somani, C. A. Avila-Orta, L. Zhu, *Phys. Rev. Lett.* **2005**, *94*, 117802.
[56] R. H. Somani, L. Yang, L. Zhu, B. S. Hsiao, *Polymer* **2005**, *46*, 8587.
[57] T. Yan, B. Zhao, Y. Cong, Y. Fang, S. Cheng, L. Li, G. Pan, Z. Wang, X. Li, F. Bian, *Macromolecules* **2009**, *43*, 602.
[58] H. Yang, D. Liu, J. Ju, J. Li, Z. Wang, G. Yan, Y. Ji, W. Zhang, G. Sun, L. Li, *Macromolecules* **2016**, *49*, 9080.
[59] P. G. Degennes, *J. Chem. Phys.* **1974**, *60*, 5030.
[60] K. P. Cui, L. P. Meng, N. Tian, W. Q. Zhou, Y. P. Liu, Z. Wang, J. He, L. B. Li, *Macromolecules* **2012**, *45*, 5477.
[61] H. Murase, Y. Ohta, T. Hashimoto, *Macromolecules* **2011**, *44*, 7335.
[62] T. Hashimoto, H. Murase, Y. Ohta, *Macromolecules* **2010**, *43*, 6542.
[63] Y. Nie, Y. Zhao, G. Matsuba, W. Hu, *Macromolecules* **2018**, *52*, 480.
[64] S. Kimata, T. Sakurai, Y. Nozue, T. Kasahara, N. Yamaguchi, T. Karino, M. Shibayama, J. A. Kornfield, *Science* **2007**, *316*, 1014.
[65] Z. Ma, L. Fernandez-Ballester, D. Cavallo, T. Gough, G. W. M. Peters, *Macromolecules* **2013**, *46*, 2671.
[66] B. Shen, Y. R. Liang, J. A. Kornfield, C. C. Han, *Macromolecules* **2013**, *46*, 1528.
[67] D. Liu, N. Tian, N. D. Huang, K. P. Cui, Z. Wang, T. T. Hu, H. R. Yang, X. Y. Li, L. B. Li, *Macromolecules* **2014**, *47*, 6813.
[68] Z. Wang, J. Ju, J. Yang, Z. Ma, D. Liu, K. Cui, H. Yang, J. Chang, N. Huang, L. Li, *Sci. Rep.* **2016**, *6*, 32968.
[69] J. Ju, Z. Wang, F. Su, Y. Ji, H. Yang, J. Chang, S. Ali, X. Li, L. Li, *Macromol. Rapid Commun.* **2016**, *37*, 1441.
[70] Z. Wang, J. Ju, L. Meng, N. Tian, J. Chang, H. Yang, Y. Ji, F. Su, L. Li, *Soft Matter* **2017**, *13*, 3639.
[71] D. Liu, N. Tian, N. Huang, K. Cui, Z. Wang, T. Hu, H. Yang, X. Li, L. Li, *Macromolecules* **2014**, *47*, 6813.
[72] F. Su, W. Zhou, X. Li, Y. Ji, K. Cui, Z. Qi, L. Li, *Macromolecules* **2014**, *47*, 4408.
[73] Z. Ma, L. Balzano, G. W. Peters, *Macromolecules* **2016**, *49*, 2724.
[74] Z. Ma, L. Balzano, T. V. Erp, G. Portale, G. W. M. Peters, *Macromolecules* **2013**, *46*, 9249.
[75] Z. Ma, L. Balzano, G. W. M. Peters, *Macromolecules* **2012**, *45*, 4216.
[76] D. Cavallo, F. Azzurri, L. Balzano, S. S. Funari, G. C. Alfonso, *Macromolecules* **2010**, *43*, 9394.
[77] F. Azzurri, G. C. Alfonso, *Macromolecules* **2005**, *38*, 1723.
[78] T. Kanaya, I. A. Polec, T. Fujiwara, R. Inoue, K. Nishida, T. Matsuura, H. Ogawa, N. Ohta, *Macromolecules* **2013**, *46*, 3031.
[79] M. N. Tamashiro, P. Pincus, *Phys. Rev. E* **2001**, *63*, 021909.
[80] G. Matsuba, Y. F. Zhao, M. Teratani, Y. Hayashi, Y. Takayama, Y. Ogino, K. Nishida, T. Kanaya, *Kobunshi Ronbunshu* **2009**, *66*, 419.
[81] Y. Zhao, K. Hayasaka, G. Matsuba, H. Ito, *Macromolecules* **2013**, *46*, 172.
[82] F. Su, Y. Ji, L. Meng, Z. Wang, Z. Qi, J. Chang, J. Ju, L. Li, *Macromolecules* **2017**, *50*, 1991.
[83] H. An, B. Zhao, Z. Ma, C. Shao, X. Wang, Y. Fang, L. Li, Z. Li, *Macromolecules* **2007**, *40*, 4740.
[84] H. An, X. Li, Y. Geng, Y. Wang, X. Wang, L. Li, Z. Li, C. Yang, *J. Phys. Chem. B* **2008**, *112*, 12256.
[85] Y. Geng, G. Wang, Y. Cong, L. Bai, L. Li, C. Yang, *Macromolecules* **2009**, *42*, 4751.
[86] T. Yamamoto, *Macromolecules* **2014**, *47*, 3192.
[87] X.-H. Dong, C.-H. Hsu, Y. Li, H. Liu, J. Wang, M. Huang, K. Yue, H.-J. Sun, C.-L. Wang, X. Yu, W.-B. Zhang, B. Lotz, S. Z. D. Cheng, Supramolecular Crystals and Crystallization with Nanosized Motifs of Giant Molecules. in *Polymer Crystallization I: From Chain Microstructure to Processing*, (Eds: F. Auriemma, G. C. Alfonso, C. de Rosa), Springer International Publishing, Cham **2017**, p. 183.
[88] F. S. Bates, G. H. Fredrickson, *Annu. Rev. Phys. Chem.* **1990**, *41*, 525.
[89] F. S. Bates, G. H. Fredrickson, *Phys. Today* **1999**, *52*, 32.
[90] S. Fischer, A. Exner, K. Zielske, J. Perlich, S. Deloudi, W. Steurer, P. Lindner, S. Forster, *Proc. Natl. Acad. Sci. U. S. A.* **2011**, *108*, 1810.
[91] C. M. Bates, T. Seshimo, M. J. Maher, W. J. Durand, J. D. Cushen, L. M. Dean, G. Blachut, C. J. Ellison, C. G. Willson, *Science* **2012**, *338*, 775.
[92] C. M. Bates, M. J. Maher, D. W. Janes, C. J. Ellison, C. G. Willson, *Macromolecules* **2013**, *47*, 2.
[93] C. Sinturel, F. S. Bates, M. A. Hillmyer, *ACS Macro Lett.* **2015**, *4*, 1044.
[94] B. van Genabeek, B. F. M. de Waal, M. M. J. Gosens, L. M. Pitet, A. R. A. Palmans, E. W. Meijer, *J. Am. Chem. Soc.* **2016**, *138*, 4210.
[95] B. van Genabeek, B. A. G. Lamers, B. F. M. de Waal, M. H. C. van Son, A. R. A. Palmans, E. W. Meijer, *J. Am. Chem. Soc.* **2017**, *139*, 14869.
[96] W.-B. Zhang, X. Yu, C.-L. Wang, H.-J. Sun, I. F. Hsieh, Y. Li, X.-H. Dong, K. Yue, R. Van Horn, S. Z. D. Cheng, *Macromolecules* **2014**, *47*, 1221.
[97] X. Yu, K. Yue, I.-F. Hsieh, Y. Li, X.-H. Dong, C. Liu, Y. Xin, H.-F. Wang, A.-C. Shi, G. R. Newkome, R.-M. Ho, E.-Q. Chen, W.-B. Zhang, S. Z. D. Cheng, *Proc. Natl. Acad. Sci. U. S. A.* **2013**, *110*, 10078.
[98] K. Yue, M. Huang, R. L. Marson, J. He, J. Huang, Z. Zhou, J. Wang, C. Liu, X. Yan, K. Wu, Z. Guo, H. Liu, W. Zhang, P. Ni, C. Wesdemiotis, W.-B. Zhang, S. C. Glotzer, S. Z. D. Cheng, *Proc. Natl. Acad. Sci. U. S. A.* **2016**, *113*, 14195.
[99] M. Huang, K. Yue, J. Huang, C. Liu, Z. Zhou, J. Wang, K. Wu, W. Shan, A.-C. Shi, S. Z. D. Cheng, *ACS Nano* **2018**, *12*, 1868.
[100] H. Liu, C.-H. Hsu, Z. Lin, W. Shan, J. Wang, J. Jiang, M. Huang, B. Lotz, X. Yu, W.-B. Zhang, K. Yue, S. Z. D. Cheng, *J. Am. Chem. Soc.* **2014**, *136*, 10691.
[101] H. Liu, J. Luo, W. Shan, D. Guo, J. Wang, C.-H. Hsu, M. Huang, W. Zhang, B. Lotz, W.-B. Zhang, T. Liu, K. Yue, S. Z. D. Cheng, *ACS Nano* **2016**, *10*, 6585.
[102] M. Huang, C.-H. Hsu, J. Wang, S. Mei, X. Dong, Y. Li, M. Li, H. Liu, W. Zhang, T. Aida, W.-B. Zhang, K. Yue, S. Z. D. Cheng, *Science* **2015**, *348*, 424.
[103] W. Zhang, M. Huang, H. Su, S. Zhang, K. Yue, X. H. Dong, X. Li, H. Liu, S. Zhang, C. Wesdemiotis, B. Lotz, W. B. Zhang, Y. Li, S. Z. Cheng, *ACS Cent. Sci.* **2016**, *2*, 48.
[104] X.-H. Dong, B. Ni, M. Huang, C.-H. Hsu, Z. Chen, Z. Lin, W.-B. Zhang, A.-C. Shi, S. Z. D. Cheng, *Macromolecules* **2015**, *48*, 7172.
[105] X. Yu, K. Yue, I. F. Hsieh, Y. Li, X. H. Dong, C. Liu, Y. Xin, H. F. Wang, A. C. Shi, G. R. Newkome, R. M. Ho, E. Q. Chen, W. B. Zhang, S. Z. Cheng, *Proc. Natl. Acad. Sci. U. S. A.* **2013**, *110*, 10078.
[106] Z. Lin, J. Sun, Y. Zhou, Y. Wang, H. Xu, X. Yang, H. Su, H. Cui, T. Aida, W. Zhang, S. Z. D. Cheng, *J. Am. Chem. Soc.* **2017**, *139*, 5883.
[107] C.-H. Hsu, K. Yue, J. Wang, X.-H. Dong, Y. Xia, Z. Jiang, E. L. Thomas, S. Z. D. Cheng, *Macromolecules* **2017**, *50*, 7282.
[108] X. Yu, W.-B. Zhang, K. Yue, X. Li, H. Liu, Y. Xin, C.-L. Wang, C. Wesdemiotis, S. Z. D. Cheng, *J. Am. Chem. Soc.* **2012**, *134*, 7780.
[109] Z. Lin, P. Lu, C.-H. Hsu, K. Yue, X.-H. Dong, H. Liu, K. Guo, C. Wesdemiotis, W.-B. Zhang, X. Yu, S. Z. D. Cheng, *Chem. A Eur. J.* **2014**, *20*, 11630.
[110] K. Yue, C. Liu, K. Guo, X. Yu, M. Huang, Y. Li, C. Wesdemiotis, S. Z. D. Cheng, W.-B. Zhang, *Macromolecules* **2012**, *45*, 8126.
[111] K. Yue, C. Liu, M. Huang, J. Huang, Z. Zhou, K. Wu, H. Liu, Z. Lin, A.-C. Shi, W.-B. Zhang, S. Z. D. Cheng, *Macromolecules* **2017**, *50*, 303.
[112] Z. Lin, P. Lu, C.-H. Hsu, J. Sun, Y. Zhou, M. Huang, K. Yue, B. Ni, X.-H. Dong, X. Li, W.-B. Zhang, X. Yu, S. Z. D. Cheng, *Macromolecules* **2015**, *48*, 5496.
[113] M. Huang, K. Yue, J. Wang, C. H. Hsu, L. Wang, S. Z. D. Cheng, *Sci. China Chem.* **2018**, *61*, 33.
[114] G. Ungar, Y. Liu, X. Zeng, V. Percec, W. D. Cho, *Science* **2003**, *299*, 1208.
[115] X. Zeng, G. Ungar, Y. Liu, V. Percec, A. E. Dulcey, J. K. Hobbs, *Nature* **2004**, *428*, 157.
[116] G. Ungar, X. Zeng, *Soft Matter* **2005**, *1*, 95.
[117] S. Lee, M. J. Bluemle, F. S. Bates, *Science* **2010**, *330*, 349.

[118] S. Lee, C. Leighton, F. S. Bates, *Proc. Natl. Acad. Sci. U. S. A.* **2014**, *111*, 17723.
[119] S. D. Hudson, V. Percec, G. Ungar, *Science* **1997**, *278*, 449.
[120] J. Zhang, F. S. Bates, *J. Am. Chem. Soc.* **2012**, *134*, 7636.

AUTHOR BIOGRAPHIES

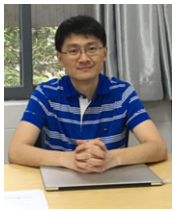

Kan Yue received his Ph.D. degree in polymer science from The University of Akron (2013) and B.S. degree in chemistry from Peking University (2008). After postdoctoral training at The University of Akron (2014) and the Brigham and Women's Hospital, Harvard Medical School (2014-2016), he joined the South China Advanced Institute for Soft Matter Science and Technology (AISMST) at the South China University of Technology (SCUT) in January 2017 to start his independent career. His research interests include macromolecular self-assembly and polymeric biomaterials.

Gengxin Liu received Ph.D. from Department of Polymer Science, University of Akron (2015) and B.S. from Department of Polymer Science and Engineering, University of Science and Technology of China (2010). His professorship started at Center for Advanced Low-dimensional Materials at Donghua University, Shanghai, China (2018).His research group (softmatters.org) works on the dynamics of giant molecules and clusters and nonlinear rheology of entangled polymers and its application.

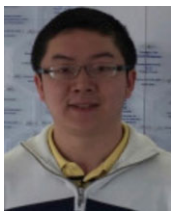

Xueyan Feng received his B.S. degree from Department of Chemistry, University of Science and Technology of China in 2011, and his Ph.D. degree from Department of Polymer Science, University of Akron in 2017. He is currently a postdoctoral researcher at Rice University. His research topic focuses on precise synthesis and self-assembly of functionalized polyhedral oligomeric silsesquioxanes based giant molecules.

Liangbin Li received his B.S. (1994) from Sichuan Normal University and M.S. (1997) from Sichuan University in Physics and his Ph.D. (2000) in Polymer Material Processing from Sichuan University. From 2000 to 2004, he was a postdoctoral fellow in FOM-Institute for Atomic and Molecular Physics and Technology University of Delft, the Netherlands. From 2004 to 2006, he worked as a Material Scientist in Unilever Food and Health Research Institute. Since 2006, taking the "one-hundred talent program" of Chinese Academy of Science, Dr. Li joined National Synchrotron Radiation Lab in University of Science and Technology of China as a full professor and started the Soft Matter Group. His primary research interests are polymer physics relevant to processing such as flow-induced crystallization of polymer and stress-induced deformation and phase transition of crystalline polymer.

Bernard Lotz was born in Alsace, France, where he has spent most of his research career at the Centre de Recherches sur les Macromolecules, which became later the Institut Charles Sadron (ICS), a laboratory owned and run by the French Centre National de la Recherche Scientifique (CNRS). He is currently Emeritus Directeur de Recherche at CNRS. He has held various positions as visiting scientist and visiting professor at several American and Japanese Universities and Research Institutes. His research interests include the phase transitions, structure and morphology of crystalline polymers and biopolymers, and block copolymers. He has authored or coauthored over 300 research articles, reviews, and book chapters.

Stephen Z. D. Cheng received his Ph.D. degree at Rensselaer Polytechnic Institute at Troy, NY, in 1985. His research interests are in the area of chemistry, physics, and engineering of polymers and advanced functional materials including ordered structure, morphology, phase transition thermodynamics, kinetics, and molecular motions. He is the recipient of Presidential Young Investigator Award (1991), John H. Dillon Medal (APS, 1995), Mettler-Toledo Award (NATAS, 1999), TA-Instrument Award (ICTAC, 2004), PMSE Cooperative Research Award (ACS, 2005), Polymer Physics Prize (APS, 2013), SPSJ International Award (Society of Polymer Science, Japan, 2017), and other awards and recognitions. Cheng has been a Fellow of AAAS and APS and an Honorable Fellow of Chinese Chemical Society. He has been elected as a member of the National Academic of Engineering of United States (2008).

How to cite this article: Yue K, Liu G, Feng X, Li L, Lotz B, Cheng SZD. A few rediscovered and challenging topics in polymer crystals and crystallization. *Polymer Crystallization*. 2018; e10053. https://doi.org/10.1002/pcr2.10053